EMBRY-RIDDLE
Aeronautical University™
SCHOLARLY COMMONS

Physical Sciences - Daytona Beach

College of Arts & Sciences

2002

Atmospheric Stability and Gravity Wave Dissipation in the Mesopause Region

Chester S. Gardner

Yucheng Zhao

Alan Z. Liu
Embry Riddle Aeronautical University - Daytona Beach, liuz2@erau.edu

Follow this and additional works at: https://commons.erau.edu/db-physical-sciences

Part of the Physical Sciences and Mathematics Commons

Atmospheric stability and gravity wave dissipation in the mesopause region

Chester S. Gardner[a],[*], Yucheng Zhao[b], Alan Z. Liu[a]

[a] *Department of Electrical and Computer Engineering, University of Illinois at Urbana-Champaign, Urbana, IL 61801, USA*
[b] *Space Physics Research Laboratory, University of Michigan, USA*

Abstract

High-resolution temperature profile data collected at the Urbana Atmospheric Observatory (40°N, 88°W) and Starfire Optical Range, NM (35°N, 106.5°W) with a Na lidar are used to assess the stability of the mesopause region between 80 and 105 km. The mean diurnal and annual temperature profiles demonstrate that in the absence of gravity wave and tidal perturbations, the background atmosphere is statically stable throughout the day and year. Thin layers of instability can be generated only when the combined perturbations associated with tides and gravity waves induce large vertical shears in the horizontal wind and temperature profiles. There is a region of reduced stability below the mesopause between 80 and 90 km where the temperature lapse rate is large and the buoyancy parameter N^2 is low. The vertical heat flux is maximum in this region which suggests that this is also a region of significant wave dissipation. There is also a region of enhanced stability above 95 km in the lower thermosphere where N^2 is large. There appears to be little wave dissipation above 95 km because the temperature variance increases rapidly with increasing altitude in this region and the vertical heat flux is zero. © 2002 Elsevier Science Ltd. All rights reserved.

Keywords: Gravity wave dissipation; Na lidar; Convective instability; Dynamic stability; Semi-diurnal tides

1. Introduction

Dissipating gravity waves transport heat, horizontal momentum, and constituents both vertically and horizontally and through such processes have a profound effect on middle atmosphere circulation, structure, and composition. Convective and dynamic instabilities are believed to play major roles in gravity wave dissipation (e.g. Hodges, 1967; Lindzen, 1981; Dewan and Good, 1986). Recent studies have shown that gravity wave instability mechanisms often include a complex combination of convective and dynamic properties (Sonmor and Klaassen, 1997). Most studies of the instability properties in the mesopause region have been limited to theoretical work, numerical simulations, and laboratory experiments (e.g. Fritts et al., 1994; Koop and McGee, 1986). Rocket probes and radars have been used to study middle atmosphere turbulence and to infer the associated eddy dissipation rates (e.g. Blix et al., 1990; Lübken et al., 1994; Lübken, 1997). Measuring stability properties of the atmosphere in the presence of gravity waves requires accurate high temporal and spatial resolution wind and temperature data. It is necessary to resolve the important waves, which can have periods as small as a few minutes, and vertical wavelengths as small as a few kilometers, and to acquire profile data with errors of not more than a few K and a few m/s. Observational studies of dynamic and static instabilities are mostly limited to the stratosphere and lower mesosphere using balloon and Rayleigh lidar observations (Sica and Thorsley, 1996; Allen and Vincent, 1995; Pfenninger et al., 1999).

In this paper, we use high-resolution temperature and wind profiles obtained at the Urbana Atmospheric Observatory (40°N, 88°W) and the Starfire Optical Range (SOR) near Albuquerque, NM (35°N, 106.5°W) to study the stability of the mesopause region between 80 and 105 km and

* Corresponding author. Fax: +1-217-244-4770.
E-mail address: cgardner@uillinois.edu (C. S. Gardner).

its influence on gravity wave dissipation. We show that the mesopause region is characterized by a region of reduced stability just below the mesopause between 80 and 90 km. Waves are most susceptible to dissipation in this region because the temperature lapse rate is large. We show that the vertical heat flux, an excellent measure of wave dissipation, and the temperature variance, an excellent measure of wave energy, are both maximum near 88 km. We also show that there is a region of enhanced stability above 95 km in the lower thermosphere where the heat flux is zero and the temperature variance increases rapidly with increasing altitude.

2. Stability of the background atmosphere

The convective or static stability of the atmosphere is characterized by the square of the buoyancy frequency N defined as

$$N^2 = \frac{g}{T} \left(\frac{\partial T}{\partial z} + \frac{g}{C_p} \right), \qquad (1)$$

where g is the gravitational acceleration (9.5 m s^{-2} in the mesopause region), T is the atmospheric temperature, and $C_p = 1004$ J K^{-1} kg^{-1} is the specific heat at constant pressure. When N^2 is negative, i.e. when the atmospheric lapse rate $\Gamma = -\partial T/\partial z$ is larger than the adiabatic lapse rate $g/C_p \approx 9.5$ K km^{-1}, the atmosphere is unstable (Peixoto, 1992). Under this condition, an air parcel displaced vertically will tend to continue moving away from its equilibrium position. Small perturbations can develop and be amplified in an unstable atmosphere.

Shear or dynamic instability is induced by large vertical shears of the horizontal wind in combination with low static stability. Dynamic stability is characterized by Richardson number, Ri, which is defined as

$$Ri = \frac{N^2}{(\partial u/\partial z)^2 + (\partial v/\partial z)^2} = \frac{N^2}{S^2}, \qquad (2)$$

where u and v are the zonal and meridional wind profiles, respectively, and $S = [(\partial u/\partial z)^2 + (\partial v/\partial z)^2]^{1/2}$ is the total vertical shear of horizontal wind. The atmosphere is considered to be dynamically unstable when $0 < Ri < 1/4$ (Peixoto, 1992). Dynamic instability occurs when there is a strong wind shear and/or small static stability. For gravity waves the stability criterion given by Eq. (2) needs to be modified since waves only respond to the projection of the wind shear in their plane of propagation. Hodges (1967) pointed out that for the mean atmosphere without gravity waves, it is unlikely for the condition of dynamic instability to be satisfied. But in the presence of gravity waves, planetary waves, and tides, large vertical shears of the temperature and horizontal wind can be generated, which often results in thin layers of instability. Whenever gravity waves propagate into unstable regions, they begin to break and dissipate their

energy as turbulence (e.g. Hodges, 1967; Lindzen, 1981; Dewan and Good, 1986). This effect is most significant above 80 km in the mesopause region where the wave amplitudes and wave-induced temperature and wind shears can become very large.

The stability of the atmosphere is critically dependent on the temperature profile. Wave-induced instabilities are most likely to occur in those regions where the lapse rate ($\Gamma = -\partial T/\partial z$) is large and N^2 is low. The annual mean temperature and N^2 profiles observed at Urbana Atmospheric Observatory (40°N, 88°W) (States and Gardner, 2000a) are plotted in Fig. 1a and b. Detailed descriptions of this data set can be found in States and Gardner (2000a, b). Because the raw temperature data were averaged over the 24 h diurnal cycle and over the whole year, the profiles in Fig. 1 do not include the effects of gravity waves and tides and therefore represent the background state of the atmosphere. Note that the background atmosphere is stable ($N^2 > 0$) throughout the region between 80 and 105 km. The smallest values of N^2 occur below the mesopause where the temperature lapse rate is large. The largest values of N^2 occur above 95 km in the lower thermosphere where the temperature increases with increasing altitude.

Fig. 2a is a contour plot of the stability parameter N^2 derived from the diurnal mean temperature profiles measured at Urbana for each week of the year (States and Gardner, 2000a). These data were obtained from 1996 to 1998 and should also be representative of SOR which is only 5° south of Urbana. The data plotted in Fig. 2a exclude the affects of tides and gravity waves and illustrate that the background atmosphere is stable throughout the mesopause region between 80 and 105 km at all times of the year. However, there is a region of reduced stability (red) near 85 km altitude where N^2 is small throughout the year. The temperature lapse rate in this region is relatively large, even in mid-summer when the mesopause is located near 87 km (States and Gardner, 2000a). Fig. 2a also shows that there is a region of enhanced stability (blue) above 95 km where N^2 is large throughout the year. This region is the boundary between the mesosphere and the lower thermosphere where the temperature generally increases with increasing altitude and so the lapse rate is relatively small.

Fig. 2b is a contour plot of the stability parameter N^2 derived from the annual mean temperature profiles measured at Urbana for each hour of the day (States and Gardner, 2000b). These data exclude the effects of gravity waves but include the effects of those tidal components that have relatively stable phases throughout the year. The background atmosphere is also stable throughout the mesopause region at all times of the day. There are regions of reduced stability (red) between 80 and 85 km and between 90 and 95 km just before local sunrise where N^2 is small. The lower region of reduced stability is below the mesopause and so the lapse rate in this region is relatively large. Nighttime chemical heating by odd-H and odd-O reactions is responsible for a prominent temperature inversion layer which forms between
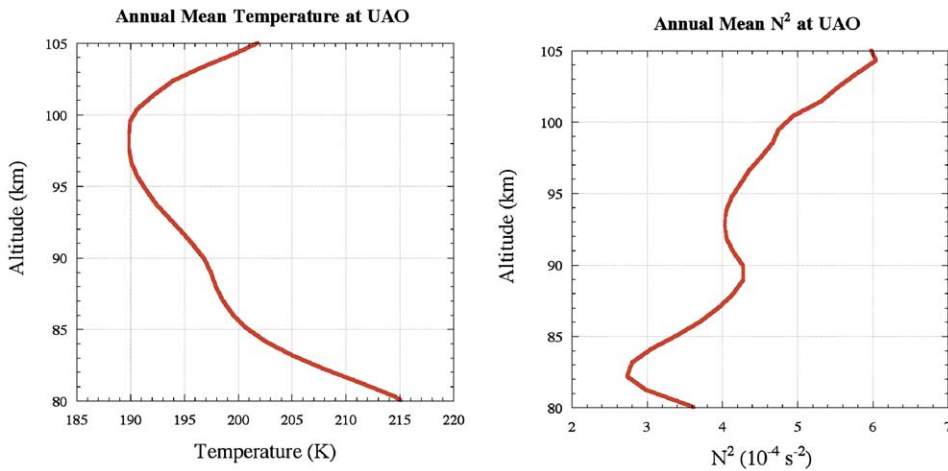
Fig. 1. (a) Annual mean temperature profile derived from more than 1000 h of Na temperature lidar observations obtained throughout the year and diurnal cycle at Urbana Atmospheric Observatory ($40°$N, $88°$W) (States and Gardner, 2000a). (b) Annual mean N^2 profile derived from the temperature profile plotted in (a).
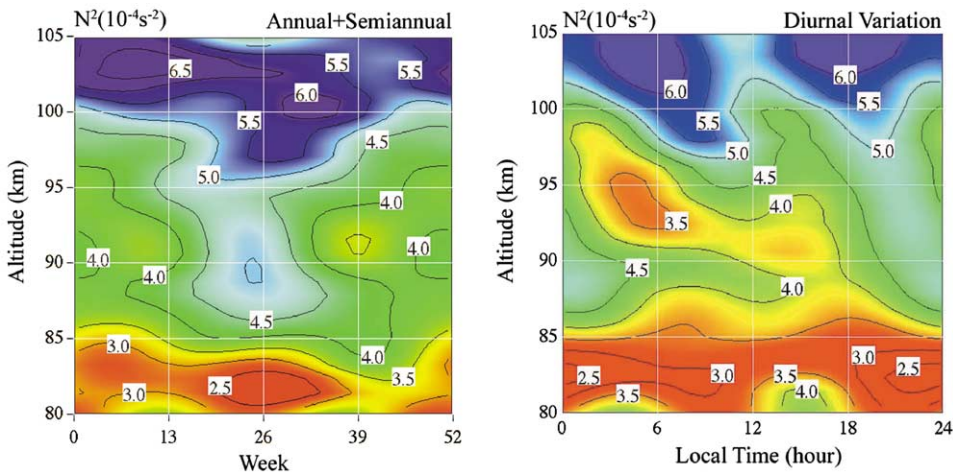

Fig. 2. (a) Contour plot of the stability parameter N^2 versus week number and altitude. The plot was derived from the diurnal mean temperature profiles collected at Urbana, IL ($40°$N, $80°$W) (States and Gardner, 2000a). (b) Contour plot of the stability parameter N^2 versus local time and altitude. The plot was derived from the annual mean temperature profiles collected at Urbana, IL ($40°$N, $80°$W) (States and Gardner, 2000b).

85 and 95 km after local midnight (Mlynczak and Solomon, 1993; States and Gardner, 2000b). The region of reduced stability between 90 and 95 km coincides with the topside of the inversion layer where the lapse rate is relatively large. In the lower thermosphere above 95 km, the temperature increases with increasing altitude and so the lapse rate is small throughout the diurnal cycle in this region of enhanced stability (large N^2).

Fig. 2 shows clearly that the background atmosphere is statically stable throughout the year and throughout the diurnal cycle even in the presence of tidal perturbations.

Dynamic instabilities can occur only if $Ri < 1/4$ or equivalently, if the total background wind shear $S > 2N$ (see Eq. (2)). The smallest value of N^2 plotted in Fig. 2 is about 2×10^{-4} s^{-2} in the region near 85 km. The background atmosphere will be dynamically unstable in this region only if the total vertical shear of horizontal winds is larger than about 30 m s^{-1} km^{-1}. Extensive MF radar observations at Urbana show that the background wind shear is well below this level throughout the year, even when the effects of tidal wind perturbations are included (Franke and Thorsen, 1993).
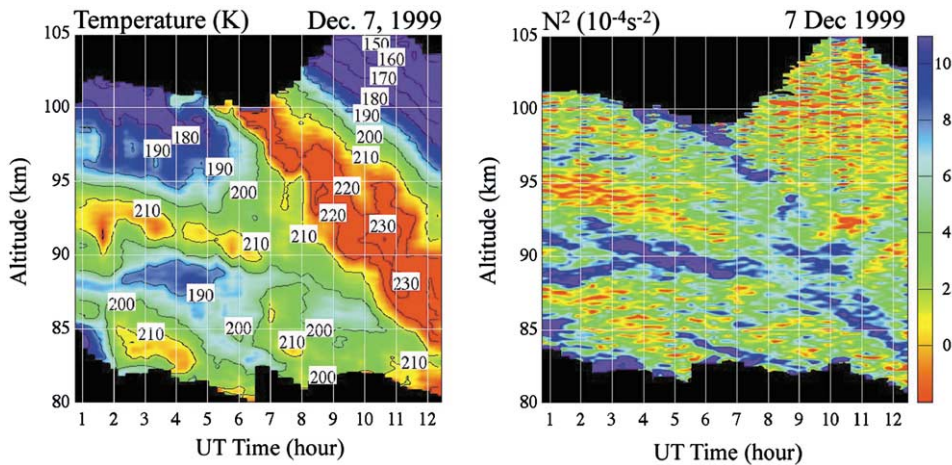
Fig. 3. (a) Contour plot of the absolute temperature measured on the night of 7 December 1999 at the Starfire Optical Range, NM (35°N, 106.5°W). The large temperature perturbations with downward phase progression are caused by the semidiurnal tide. (b) Contour plot of N^2 for the night of 7 December 99. Red and orange corresponds to regions where the atmosphere is statically unstable ($N^2 < 0$). Cooler colors represent progressively larger positive values of N^2.

3. Stability of the atmosphere in the presence of gravity waves

Tides alone are usually not sufficient to induce static or dynamic instabilities. However, tides, in combination with gravity waves, can have a large impact on atmospheric stability. In the mesopause region where gravity wave amplitudes are large, instabilities appear to be quite common. Zhao et al. (2002) report that the measured probabilities of static and dynamic instabilities in the mesopause region above SOR, average 8% and 15%, respectively. To illustrate, the temperature field observed at SOR on the night of 7 December 1999 is plotted versus altitude and UT in Fig. 3a. The corresponding values of N^2 are plotted in Fig. 3b. The N^2 contours are color coded so that the statically unstable regions ($N^2 < 0$) are red and orange. Cooler colors (yellow–blue) represent progressively larger positive values of N^2. On this night, the Na wind/temperature lidar was pointed at zenith for the whole observation period to obtain the highest temporal resolution data. These contour plots were derived from temperature profiles processed with a 90 s temporal resolution and 500 m vertical resolution and so include the effects of waves with observed periods longer than 3 min and vertical wavelengths longer than 1 km. At this resolution, the rms temperature error is typically $< \pm 2$ K. In the region within ± 5 km of the peak of the Na layer near 92 km, the errors are typically $< \pm 1$ K.

The large temperature perturbation with downward phase progression that is most prominent after 0600 UT in Fig. 3a is the semidiurnal tide. The semidiurnal thermal tide has maximum amplitude in December and January when the amplitude of the diurnal tide is minimum (States and

Gardner, 2000b). On this night, the statically unstable regions are highly correlated with these tidal oscillations. They occur primarily on the topside of the tidal perturbations where the temperature decreases with increasing altitude and the lapse rate is large and in the region around 85 km where the background value of N^2 is small at all times of the day and year. In these regions, the temperature perturbations associated with the gravity waves are sufficient to drive the lapse rate into the super-adiabatic regime so that N^2 becomes negative and the atmosphere is statically unstable. Note that the unstable layers are typically 1–2 km thick and persist for a few tens of minutes to more than an hour. They appear to be caused primarily by the short vertical wavelength waves (< 5 km). Another example of the combined effects of gravity waves and tides on the stability of the mesopause region can be found in Zhao et al. (2002).

4. Heat flux and temperature variance profiles

The vertical flux of heat is defined as the expected value of the product of the vertical wind (w') and temperature (T') perturbations $\langle w'T' \rangle$ (angle brackets denote ensemble average). In the absence of wave dissipation, the wave perturbations in temperature are proportional to vertical displacement so that w' and T' are orthogonal, and the vertical heat flux is zero. Dissipation mechanisms such as saturation, diffusive damping, critical layer interactions, and instabilities alter the phase relationship between the wave-induced vertical wind and temperature perturbations, thus giving rise to a net heat transport and a nonzero value for the heat flux. Therefore, the vertical heat flux profile is an excellent
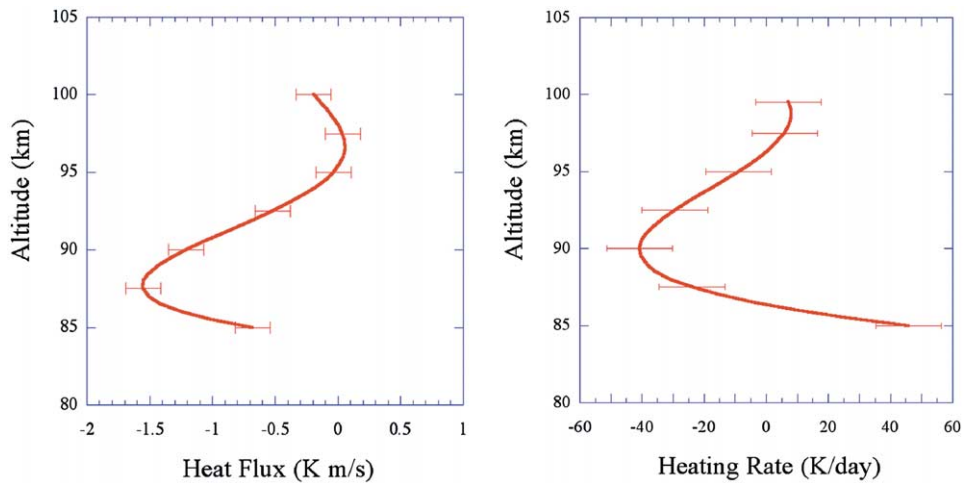
Fig. 4. (a) Annual mean vertical heat flux profile derived from 200 h of Na wind/temperature lidar data collected during the nighttime at Starfire Optical Range, NM since January 1998. (b) Heating (Cooling) rate profile derived from the heat flux profile plotted in (a). Negative values imply cooling.

measure of wave dissipation. Several authors have explored the relationship between gravity wave dissipation and the vertical heat flux and have shown that dissipating waves typically transport heat downward (e.g., Walterscheid, 1981; Weinstock, 1983). This can result in substantial cooling as heat is transported to lower altitudes.

The annual mean vertical heat flux and heating (cooling) rate profiles, derived from more than 200 h of vertical wind and temperature data collected by the University of Illinois Na lidar at SOR from June 1998 till April 2000, are plotted in Fig. 4. The wind and temperature profiles were first processed with a vertical resolution of 500 m and a temporal resolution of 90 s. The wind and temperature perturbations were then computed by subtracting a linear trend in time at each altitude, as well the mean between 85 and 100 km. The average observation period was about 8 h. The resulting vertical wind and temperature perturbations, heat flux, and cooling rate profiles include the affects of waves with periods between about 3 min and 16 h and vertical wavelengths between about 1 and 30 km. A detailed discussion of the heat flux observation technique and error analysis can be found in Gardner and Yang (1998). Zhao et al. (2002) provide a detailed description of the SOR lidar data used in this paper and its accuracy.

The mean heat flux is maximum (downward) near 88 km, just above the region of reduced stability (red) illustrated by the N^2 contours plotted in Fig. 2. The mean heat flux is nearly zero above 95 km in the region of enhanced stability (blue) in the lower thermosphere where the background temperature increases monotonically with increasing altitude. The heat flux profile suggests that wave dissipation is significant between 85 and 93 km, just above the region between 80 and 85 km where the values of N^2 for the background
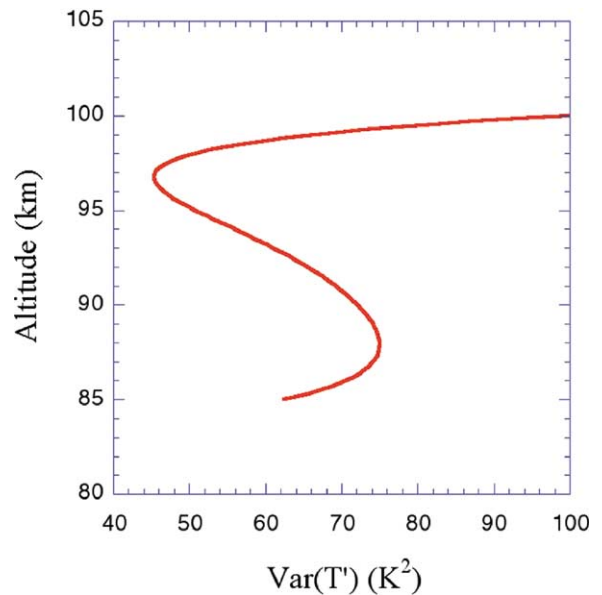

Fig. 5. Temperature variance profile derived from 200 h of Na wind/temperature lidar data collected during the nighttime at Starfire Optical Range, NM since January 1998.

atmosphere are lowest. Conversely, dissipation is virtually nonexistent above 95 km where N^2 is largest. The values of the observed heat flux and heating (cooling) rate are consistent with theoretical predictions for this region of the mesosphere (Walterscheid, 1981; Weinstock, 1983; Gardner and Yang, 1998).

The temperature variance profile derived from this same data set is plotted in Fig. 5. The gravity wave temperature

variance is proportional to the total horizontal wind variance. In the absence of dissipation, the variance increases as the waves propagate to higher altitudes in response to decreasing atmospheric density. When the waves are dissipating, the variance increases more slowly with increasing altitude and can even decrease when the dissipation is severe. The temperature variance profile plotted in Fig. 5 also suggests that the waves experience severe dissipation in the region between 80 and 90 km where the stability of the background atmosphere is lowest (i.e. N^2 is lowest) and the heat flux is maximum. The variance reaches a local maximum near 88 km and then decreases monotonically, reaching a local minimum just above 95 km. Above 95 km, where the heat flux is zero and N^2 is largest, the variance increases rapidly with increasing altitude as expected in the absence of dissipation.

5. Conclusions

It has long been recognized that gravity wave saturation and dissipation processes play a dominant role in maintaining the general circulation of the middle atmosphere. Dissipating waves transport heat, horizontal momentum, and constituents and through such processes have a profound effect on middle atmosphere structure and composition. Dissipation depends critically on atmospheric stability. The background atmosphere is expected to be stable both statically and dynamically even in the presence of tides. However, in the mesopause region where gravity waves can achieve high amplitudes, the combined effects of the background temperature profile, tides, and gravity waves can induce sufficiently large vertical shears in the horizontal wind and temperature profiles so that the atmosphere becomes unstable and the waves begin to dissipate.

We have shown that the mesopause region between 80 and 105 km is characterized by a region of reduced stability between 80 and about 90 km where the stability parameter N^2 is low. It is also characterized by a region of enhanced stability above 95 km in the lower thermosphere where N^2 is large. Wave dissipation is most significant just below the mesopause between 80 and 90 km where the wave amplitudes are large. The heat flux, which is an excellent measure of wave dissipation, and the temperature variance, a measure of wave energy, are both maximum at 88 km. Because of dissipation the wave amplitudes decrease above 88 km reaching a local minimum just above 95 km. Dissipation is negligible above 95 km where the heat flux is zero and as a consequence, the temperature variance increases rapidly with increasing altitude. N^2, heat flux, and temperature variance profiles are all consistent with the hypothesis that wave dissipation is most significant between 80 and 90 km where the mean value of N^2 is smallest. They are also consistent with the assumption that dissipation is negligible in the lower thermosphere above 95 km where N^2 is large.

References

Allen, S.J., Vincent, R.A., 1995. Gravity wave activity in the lower atmosphere: seasonal and latitudinal variations. Journal of Geophysical Research 100, 1327–1350.

Blix, T.A., Thrane, E.V., Fritts, D.C., von Zahn, U., Lübken, F.-J., Hillert, W., Blood, S.P., Mitchell, J.D., Kokin, G.A., Pakhomov, S.V., 1990. Small-scale structure observed in-situ during MAC/EPSILON. Journal of Atmospheric Terrestrial Physics 52, 835–854.

Dewan, E.M., Good, R.E., 1986. Saturation and the "universal" spectrum for vertical profiles of horizontal scalar winds in the atmosphere. Journal of Geophysical Research 91, 2742–2748.

Franke, S.J., Thorsen, D., 1993. Mean winds and tides in the upper middle atmosphere at Urbana (40°N, 88°W) during 1991–1992. Journal of Geophysical Research 98, 18,607–18,615.

Fritts, D.C., Isler, J.R., Andreassen, Ø., 1994. Gravity wave breaking in two and three dimensions, 2, Three-dimensional evolution and instability structure. Journal of Geophysical Research 99, 8109–8123.

Gardner, C.S., Yang, W., 1998. Measurements of the dynamical cooling rate associated with the vertical transport of heat by dissipating gravity waves in the mesopause region at the Starfire Optical Range, NM. Journal of Geophysical Research 103, 16,909–16,927.

Hodges Jr., R.R., 1967. Generation of turbulence in the upper atmosphere by internal gravity waves. Journal of Geophysical Research 72, 3455–3458.

Koop, C.G., McGee, B., 1986. Measurements of internal gravity waves in a continuously stratified shear flow. Journal of Fluid Mechanics 172, 453.

Lindzen, R.S., 1981. Turbulence and stress owing to gravity wave and tidal breakdown. Journal of Geophysical Research 86, 9707–9714.

Lübken, F.-J., 1997. Seasonal variation of turbulent energy dissipation rates at high latitudes as determined by in situ measurements of neutral density fluctuations. Journal of Geophysical Research 102, 13,441–13,456.

Lübken, F.-J., Hillert, W., Lehmacher, G., von Zahn, U., Blix, T.A., Thrane, E.V., Widdel, H.-U., Kokin, G.A., Knayazev, A.K., 1994. Morphology and sources of turbulence in the mesosphere during DYANA. Journal of Atmospheric Terrestrial Physics 56, 1809–1833.

Mlynczak, M.G., Solomon, S., 1993. A detailed evaluation of heating efficiency in the middle atmosphere. Journal of Geophysical Research 98, 10,517–10,541.

Peixoto, J.P., 1992. Physics of Climate. American Institute of Physics, New York, 520pp.

Pfenninger, M., Liu, A.Z., Papen, G.C., Gardner, C.S., 1999. Gravity wave characteristics in the lower atmosphere at south pole. Journal of Geophysical Research 104, 5963–5984.

Sica, R.J., Thorsley, M.D., 1996. Measurements of superadiabatic lapse rates in the middle atmosphere. Geophysical Research Letters 23, 2797–2800.

Sonmor, L.J., Klaassen, G.P., 1997. Toward a unified theory of gravity wave stability. Journal of the Atmospheric Sciences 54, 2655–2680.

States, R.J., Gardner, C.S., 2000a. Thermal structure of the mesopause region (80–105 km) at 40°N latitude. Part I: Seasonal variations. Journal of the Atmospheric Sciences 57, 66–77.

States, R.J., Gardner, C.S., 2000b. Thermal structure of the mesopause region (80–105 km) at 40°N latitude. Part II: Diurnal variations. Journal of the Atmospheric Sciences 57, 78–92.

Walterscheid, R.L., 1981. Dynamical cooling induced by dissipating internal gravity waves. Geophysical Research Letters 8, 1235–1238.

Weinstock, J., 1983. Heat flux induced by gravity waves. Geophysical Research Letters 10, 165–167.

Zhao, Y., Liu, A., Gardner, C.S., 2002. Measurements of atmospheric stability in the mesopause region at Starfire Optical Range, NM, submitted to Journal of Atmospheric and Solar-Terrestrial Physics.